BULETINUL Universităţii Petrol – Gaze din Ploieşti	Vol. LXVIII No. 1/2016	87 – 96	Seria Tehnică

Analysis of Deformations Caused by Corrosion of Metal Construction of Excavator Arm ERC 1400

Dan Dobrotă, Cătălin Iancu

”Constantin Brâncuşi” University of Târgu-Jiu, Engineering Faculty, Geneva Street, nr. 3, Târgu-Jiu
e-mail: ddan@utgjiu.ro

Abstract

The corrosion problem of metal constructions of mining machinery is a very complex one, because of the environmental conditions in which they work. The paper presents results of experimental research which aimed to identify the corrosion of main elements of the 1400 ERC excavator arm. Corrosion size was determined using Leptoskop type equipment that allowed determining the thickness of the oxide layers and painting also. In parallel with the results obtained in the experimental research was carried out also a FEM analysis to identify the stresses and deformations of steel construction. Results permit establishing lifetime reserve of welded metal construction of the excavator port ladder arm.

Key words: *metal construction, corrosion, FEM analysis, lifetime*

Introduction

Extending life for welded structures is possible through constructive improvements and development of new technological processes, for intervention and repair. Thus, research is needed on areas of welded assemblies that may damage in operation especially due to the emergence corrosion cracking phenomenon [1].

Structural changes and technological research testing aim to remove and prevent nonconformities occur in service, the most dangerous being made by welding metal construction rupture caused by corrosion cracking. Sometimes plastic deformation leads to the appearance of cracks, whose size depends on the effort and the application thereof. For welded structures, temperature execution generates conditions for certain ways of breaking that causes in general degradation and accidental removal from service of welded structures [2].

To prevent breakage of welded construction equipment in surface exploitations is recommended that these welded steel structures be performed at temperatures above 10°C to avoid embrittlement in the area of thermal influence. Also, the operating temperature can affect the efforts that occur in the degradation of the piece obtained by welding, depending on the thickness [3].

For equipment from quarries pit lignite, the most stressed part is infrastructure which includes arm shedder excavator (fig. 1), subassembly where appeared most failures due to nonconformities whose causes is related to technology and material, and also the use of equipment in a quite corrosive environment. Arm as supporting the bucket rotor subassembly

has the strongest demand during the operation and once operational deficiencies occur, they lead inevitably to decrease projected lifetime if not proceed to repair welded structure.

Fig. 1. Excavator arm.

Welded construction degradation occurs after 5-7 years of operation and have generally causes related to how the machine functioned in heavy regimes for long periods of time [4, 5]. For quarries pit lignite machines, geological conditions and mechanisms planned repairs are causes that determine degradation of welded structure.

Materials and Methods

The choice of welding processes and filler material is primarily chosen by subassembly design and technical conditions available to the contractor. In general, for weight and large-sized assemblies made of profiles, plates and other items machined, hand-welding process with coated electrode is most common, but in recent decades has greatly expanded MAG process for welding.

The seam weld is made of filler metal and a part of the molten matrix metal, resulting in a chemically formed compound by mutual diffusion of the two components. The welded assembly of excavator arm ERC 1400 was studied, which made from sheet metal cues from OL 52.4k material (originally for two imported machinery from KRUPP - material was St 52.3), positioned and assembled by manual welding with basic electrodes. After 1994, was carried on to the welding submerged and then MAG welding in active gas environment with normal polarization wire sources and in this respect has been used as a protective environment carbon dioxide and argon combinations thereof.

The quarries of lignite surface mining in addition to actual exploitation, are spaces for storage, handling and loading. In all these places, some of lignite breaks down and as a result of relatively low rainfall appears the self-ignition phenomena. Self-ignition occurs even in the extraction zone, on excavators vehicular platforms. The ashes resulting from the combustion contains sulfur in the composition and generates carbon dioxide, which in contact with the ground water but also the precipitation, forming solution which attacks metallic structure resulting oxides. Their interactions versus paint film that protects metal construction can be from physical or chemical nature [6].

The chemical action is due to the action of naturally acidic chemical combinations that may occur in the atmosphere, but also is due to electrical effects as atmospheric electrical current leakage or electrical systems on the machine. Chemical action is fueled by some leakage current through the metal construction that transforms in real-cells specific areas in which the ccumulated action of the internal tensions and atmospheric external factors rush chemical degradation. The emergence of chemical intercrystalline cracks developed in continental climate conditions, lead to the development of intercrystalline oxides (temp. 25°- 40°C, humidity 70-80%). These steel oxides have much higher volume than steel and in such circumstances, the mechanism of corrosion cracking accelerates; danger of development of corrosion cracks under the protective film generates oxidation expansion and in its absence is fast expanding [7].

In these circumstances researches followed oxide film thickness and paint determination on metal construction elements, thus can be established the effective thickness of rolled steel elements of the steel structure. To achieve research initially have been identified the size of the excavator arm metallic structure elements and on these elements were positioned analysis points located at a distance of about 250 mm (fig. 2).

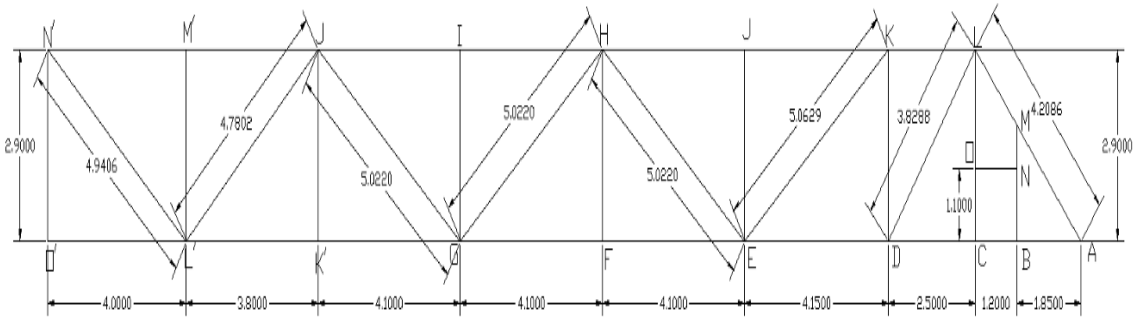

Fig. 2. Excavator arm dimensions.

Experimental Results

To achieve experimental research using was used a universal type equipment Leptoscop 2042, which allows measuring the thickness of the oxide film and paint respectively. So was measured the total thickness of metal plates of steel structure in many points with a micrometer, and from the thickness of this layer was subtracted size of oxides and paint.

To make identification more accurate, measurement of the corrosion oxide layer and paint was done on one side and the other of metallic structure for each profile. From visual analysis of the steel structure of the excavator arm were observed maximum deformations of metal structure in the KL beam (fig. 3) and thus the research was focused on identifying the wear of beams linked to this beam, respectively LC, LD and LA beams.

Fig. 3. Major deformation zone that appeared in the HL beam.

Major deformation of HL beam may be explained by the fact that it is horizontally positioned and acid water could to corrode more but also because tensions arise here are the largest due to bucket wheel stress [8]. A general view of the HL beam and metallic profile shape I300 is shown in Figure 4, and experimental research results are presented in Table 1.

Fig. 4. Beam HL and its profile

Table 1. HL beam dimensions deduced from the measurements

Beam HL								
Thickness [mm]								
Exp. no.	Front	Front without paint and oxides	Back	Back without paint and oxides	Superior	Superior without paint and oxides	Inferior	Inferior without paint and oxides
1	10.87	10.647	10.76	10.498	10.66	10.414	11.07	10.852
2	10.97	10.769	10.63	10.411	10.69	10.474	10.59	10.381
3	10.67	10.467	10.48	10.246	10.83	10.498	10.88	10.307
4	10.79	10.63	10.48	10.178	11.06	10.737	10.49	10.238
5	10.72	10.565	10.59	10.302	10.67	10.479	10.53	10.242
6	10.65	10.408	10.74	10.459	10.58	10.361	10.79	10.484
7	10.70	10.471	10.63	10.404	10.50	10.223	10.86	10.685
8	10.63	10.367	10.47	10.235	10.34	10.183	10.65	10.387
9	10.77	10.483	10.44	10.166	10.66	10.433	10.47	10.182
10	10.88	10.638	11.12	10.699	11.19	10.992	10.47	10.265
11	10.75	10.545	10.13	9.826	10.75	10.587	10.67	10.511
12	10.87	10.295	11.11	10.871	10.37	10.181	11.11	10.857
13	10.75	10.538	11.12	10.862	10.74	10.562	10.77	10.585
14	10.67	10.404	10.94	10.619	10.70	10.518	10.35	10.174
15	10.89	10.67	11.10	10.75	10.93	10.702	10.73	10.481
16	10.87	10.591	10.83	10.527	11.01	10.799	10.75	10.585
17	10.74	10.519	10.90	10.752	10.98	10.878	10.77	10.601
18	10.82	10.639	10.87	10.756	10.44	10.227	10.79	10.623

A general view of the beam AL and the shape metal profile U200 is shown in Figure 5 and experimental research results are presented in Table 2.

Fig. 5. Beam AL and its profile.

Table 2. AL beam dimensions deduced from the measurements

Beam AL					Paint thickness [μm]					
Thickness [mm]					Superior			Inferior		
Exp. no.	Superior	Superior without paint and oxides	Inferior	Inferior without paint and oxides	S_1	S_2	S_1 +S_2	S_1	S_2	S_1 +S_2
1	11.06	10.734	10.91	10.6689	219	107	326	142	99.1	241.1
2	11.17	10.975	10.92	10.7692	114	81	195	82.1	68.7	150.8
3	11.21	11.0113	10.57	10.3879	111	87.7	198.7	111	71.1	182.1
4	10.45	10.2863	10.23	10.0343	96.4	67.5	163.9	94.7	101	195.7
5	11.20	10.484	10.91	10.6261	631	85	716	150	134	284
6	10.93	10.7286	10.55	10.3688	151	50.4	201.4	79.2	102	181.2
7	10.92	10.7912	10.90	10.6744	67.5	61.3	128.8	133	92.6	225.6
8	10.61	10.4772	10.66	10.501	64.3	68.5	132.8	72.4	86.6	159
9	11.04	10.8278	10.51	10.296	140	72.2	212.2	105	109	214
10	10.96	10.793	10.32	10.066	76.7	90.3	167	124	130	254
11	11.35	11.1577	10.41	10.2187	116	76.3	192.3	86.3	105	191.3
12	10.49	10.3287	10.27	9.852	46.3	115	161.3	131	287	418

A general view of the beam AL and the shape metal profile U200 is shown in Figure 6 and experimental research results are presented in Table 3.

Fig. 6. Beam AL and its profile.

Table 3. LC beam dimensions deduced from the measurements

Beam LC					Paint thickness [μm]					
Thickness [mm]					Left			Right		
Exp. no.	Left	Left without paint and oxides	Right	Right without paint and oxides	S_1	S_2	S_1+S_2	S_1	S_2	S_1+S_2
1	10.63	10.415	10.31	10.168	88.3	127	215.3	102	40.1	142.1
2	10.42	10.209	10.52	10.3	146	65.8	211.8	105	115	220
3	10.53	10.102	10.67	10.407	151	277	428	165	98.1	263.1
4	10.63	10.181	10.29	10.069	181	268	449	97.5	124	221.5
5	10.42	10.131	10.35	10.131	127	162	289	146	73.3	219.3
6	10.44	10.074	10.40	10.289	150	216	366	54.5	57.3	111.8

A general view of the beam AL and the shape metal profile L150x100 is shown in Figure 7, and experimental research results are presented in Table 4.

Fig. 7. Beam LD and its profile.

Table 4. LD beam dimensions deduced from the measurements

Beam LD					Paint thickness [μm]					
Thickness [mm]					Front			Back		
Exp. no.	Front	Front without paint and oxides	Back	Back without paint and oxides	S_1	S_2	S_1+S_2	S_1	S_2	S_1+S_2
1	13.25	13.017	13.18	12.905	146	87.2	233.2	177	98	275
2	13.25	13.281	14.25	14.014	113	106	219	125	111	236
3	13.47	13.199	13.71	13.427	176	95.2	271.2	154	129	283
4	13.75	13.453	13.57	13.226	198	99.2	297.2	225	119	344
5	14.09	13.829	13.67	13.321	186	75.3	261.3	256	93.2	349.2
6	14.02	13.747	13.36	13.155	157	116	273	127	78.8	205.8
7	13.90	13.613	13.86	13.616	160	127	287	151	93.4	244.4
8	13.92	13.63	14.01	13.741	183	107	290	176	83.3	259.3
9	13.69	13.511	14.63	14.327	86.6	93.2	179.8	179	124	303

To confirm the results of experimental research was used also FEM for determining stress and deformation values in the metal structure of the ERC 1400 excavator arm [9]. ERC Structure 1400 is a massive spacial structure that can be studied by finite element mesh using a p-element method. First was created geometric model after considering the size measurements obtained, and then the model was meshed with tetrahedral elements of second order. These elements are used for good meshing with small errors on curved surfaces. For the FEM analysis were established boundary conditions, respectively on one end embedding and loading caused by rotor bucket on the other end.

Analysis of stresses from the arm of the excavator status ERC 1400 is presented in Figure 8.

Analysis of the excavator arm 1400 ERC deformations status resulting from FEM analysis is presented in Figure 9.

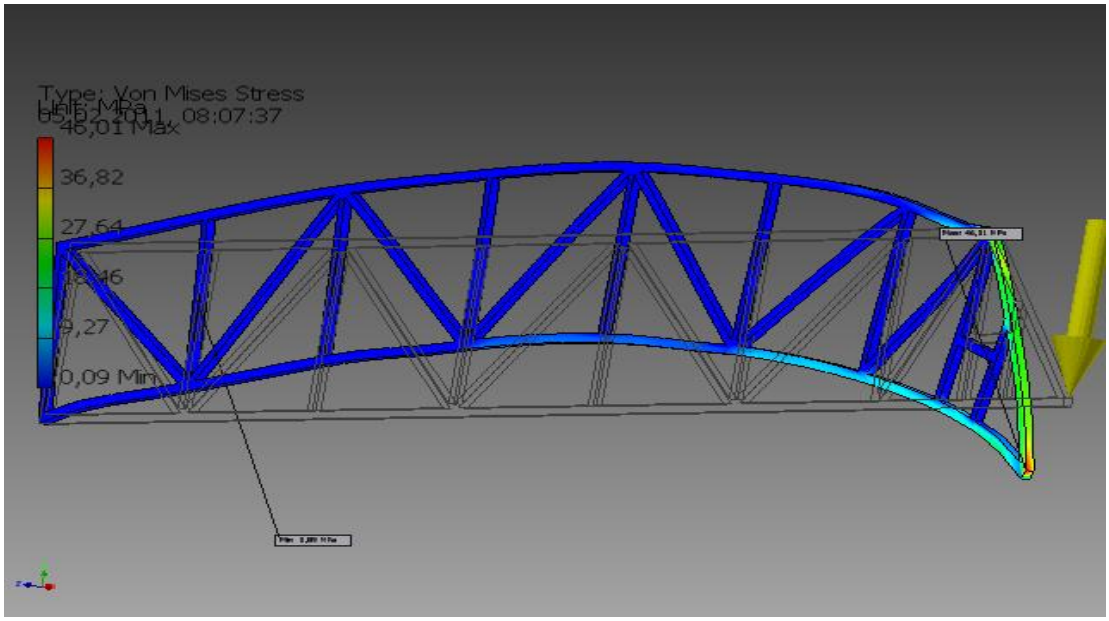

Fig. 8. Analysis of the stress of the excavator arm ERC 1400.

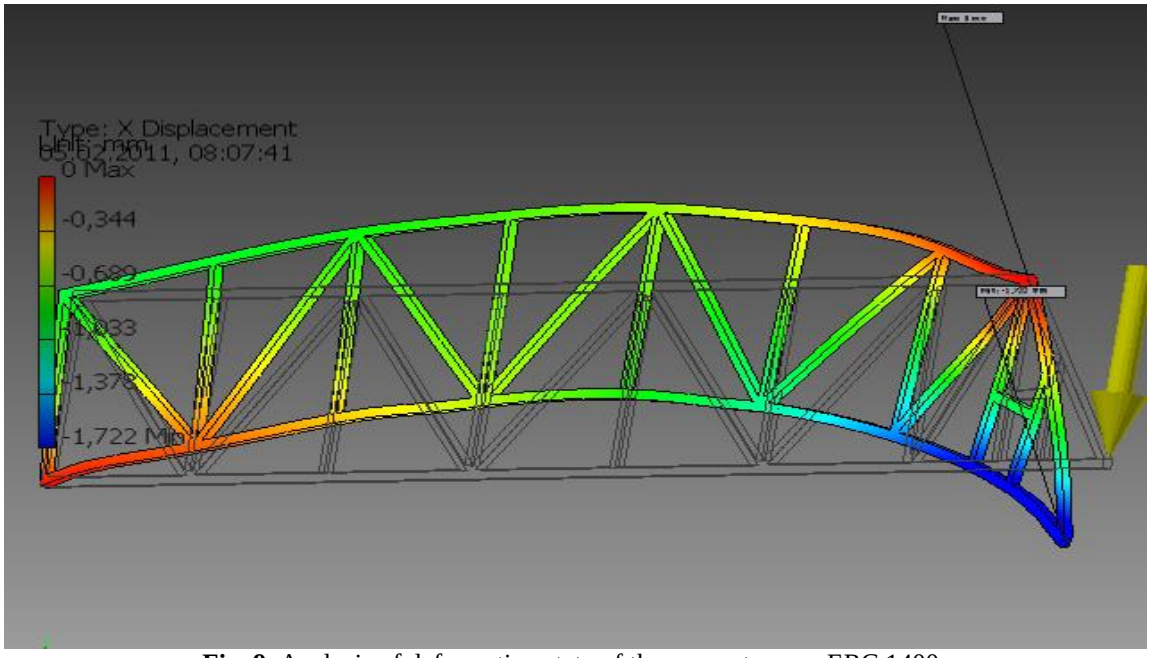

Fig. 9. Analysis of deformation state of the excavator arm ERC 1400

Conclusions

- Degradation by corrosion till the final destruction of metallic structure of the ERC 1400 excavator goes through several stages: initiation of corrosion; development of corrosion; corrosion cracks occurrence; short crack propagation; fissure transition from short to long crack, crack propagation and long cracks union;
- From visual analysis it was observed that the maximum deformation is seen on the structural elements from arm head where are mounted excavator drum shedder;
- HL beam presents the greatest redistribution of material, which makes it to be the most powerful stressed and thus for increasing the lifetime must be adopted technical solutions which allows increasing rigidity of this element;
- Use of leptoscop to measure paint thickness and oxide layers allows determining the thickness of the section of the metal beams that exists in reality after use;
- Changes in the thickness of the section of the metal beams cause a change in the state of stresses and deformations in beams and thus reduces lifetime of the steel structure of the excavator ERC 1400;
- After identifying the thickness of the section of the metal beams was performed a FEM analysis that allowed establishing real stress and deformation occurring in metallic structure;
- By using MEF is proven that deformation in reality is confirmed by the Finite Element Method analysis;
- Elements of the excavator arm having a horizontal arrangement are the most stressed implying a focus on operation and maintenance for these items;
- Elements of the excavator arm having a horizontal arrangement have the highest corrosion, and this is determined by stagnation on them of acid rain.

References

1. Stephens, R.I., Fatemi, A., Stephens, R.R., Fuchs, H.O. – *Metal Fatigue in Engineering*, Wiley, 2000.
2. Vîlceanu, F., Iancu, C. – Methodology of establishing residual lifetime of lifting installation by non-destructive methods, *Fiability and Durability*, 2013, pp.168-172.
3. * * * – SR EN ISO 13920-98: *Welding. General tolerances for welded constructions*.
4. * * * – SR EN 1993/2006: *Design of steel structures.*
5. * * * – ENV 1993-1-8: *Design of Steel Structures - General - Design of Joints.*
6. * * * – SR EN 1991/2007: *Eurocode 1: Actions on structures - Part 1-3: General actions – Loads*. National Annex.
7. Mäkeläinen, P. – *Advanced steel structures - Fatigue design*, Helsinki University of Technology, 2003.
8. Roessle, M.L., Fatemi, F. – Strain-controlled fatigue properties of steels and some simple approximations, *Int. J. Fatigue* **22**, 2000, pp.495–511.
9. Iancu, C., Dobrotă, D. – An analytical - FEA approach to lifetime estimation of mining equipments, *Proceedings of the 7th Australasian Congress on Applied Mechanics, ACAM 7*, Adelaide, Australia, December 2012, pp. 612-621.

Analiza deformaţiilor determinate de coroziunea construcţiei metalice a braţului excavatorului ERC 1400

Rezumat

Problema coroziunii construcţiilor metalica ale utilajelor miniere este una foarte complexă, datorită condiţiilor de mediu în care lucrează acestea. În cadrul lucrării sunt prezentate rezultate ale cercetărilor experimentale prin care s-a urmărit identificarea coroziunii pentru elementele principale ale braţului excavatorului ERC 1400. Mărimea coroziunii a fost stabilită cu ajutorul unui echipament de tip Leptoskop care a permis determinarea grosimii straturilor de oxizi şi de vopsea. În paralel cu rezultatele obţinute în cadrul cercetărilor experimentale a fost efectuată şi o analiză MEF pentru identificarea tensiunilor şi deformaţiilor din construcţia metalică. Rezultatele obţinute permit stabilirea rezervei de viaţă a construcţiei metalice sudate a braţului port-elindă a excavatorului.